International Journal of Fracture **106:** 81–93, 2000.

Stress analysis of arbitrarily distributed elliptical inclusions under longitudinal shear loading

NAO-AKI NODA[1] and TADATOSHI MATSUO[2]
[1]*Department of Mechanical Engineering, Kyushu Institute of Technology, Kitakyushu 804-8550, Japan*
[2]*Department of Mechanical Engineering, Fukushima National College of Technology, Iwaki 970-8034, Japan*

Received 3 May 1999; accepted in revised form 20 March 2000

Abstract. This paper deals with an interaction problem of arbitrarily distributed elliptical inclusions under longitudinal shear loading. The problem is formulated as a system of singular integral equations with Cauchy-type or logarithmic-type singularities, where unknown functions are the densities of body forces distributed in the longitudinal directions of infinite bodies having the same elastic constants as those of the matrix and inclusions. In order to satisfy the boundary conditions along the elliptical inclusions, four kinds of fundamental density functions are introduced in a similar way of previous papers treating plane stress problems. Then the body force densities are approximated by a linear combination of those fundamental density functions and polynomials. In the analysis, elastic constants of matrix and inclusion are varied systematically; then the magnitude and position of the maximum stress are shown in tables and the stress distributions along the boundary are shown in figures. For any fixed shape, size and elastic constant of inclusions, the relationships between number of inclusions and maximum stress are investigated for several arrangements.

Key words: Body force method, elasticity, elliptical inclusion, interaction effect, longitudinal shear, numerical analysis, singular integral equation stress concentration.

1. Introduction

It is well-known that most engineering materials contain some defects in the form of cracks, voids or inclusions. To evaluate the effect of defects on the strength of structures, it is important to know the stress concentration of elliptical inclusions because they cover a wide variety of particular cases, such as line and circular defects. Therefore elliptical and ellipsoidal inclusion problems are treated by many researchers [1–4]. However arbitrary distributed elliptical inclusions under longitudinal shear loading have not been treated yet. In this paper, the interaction of distributed elliptical inclusions in an infinite body under longitudinal shear is analyzed by extending the previous research [5] based on the body force method [6]. Then, the magnitude and position of the maximum stress are examined, when the shape, position and number of inclusions are varied. The results show that the introducing fundamental density functions can yield rapid converging numerical results and satisfy the boundary conditions along the entire boundary. It is also found that this method yields a smooth stress variation along the boundary with high accuracy. Also, stress concentration factor of a row of elliptical inclusions is extrapolated on the linear relationship between the maximum stress and the number of inclusions.

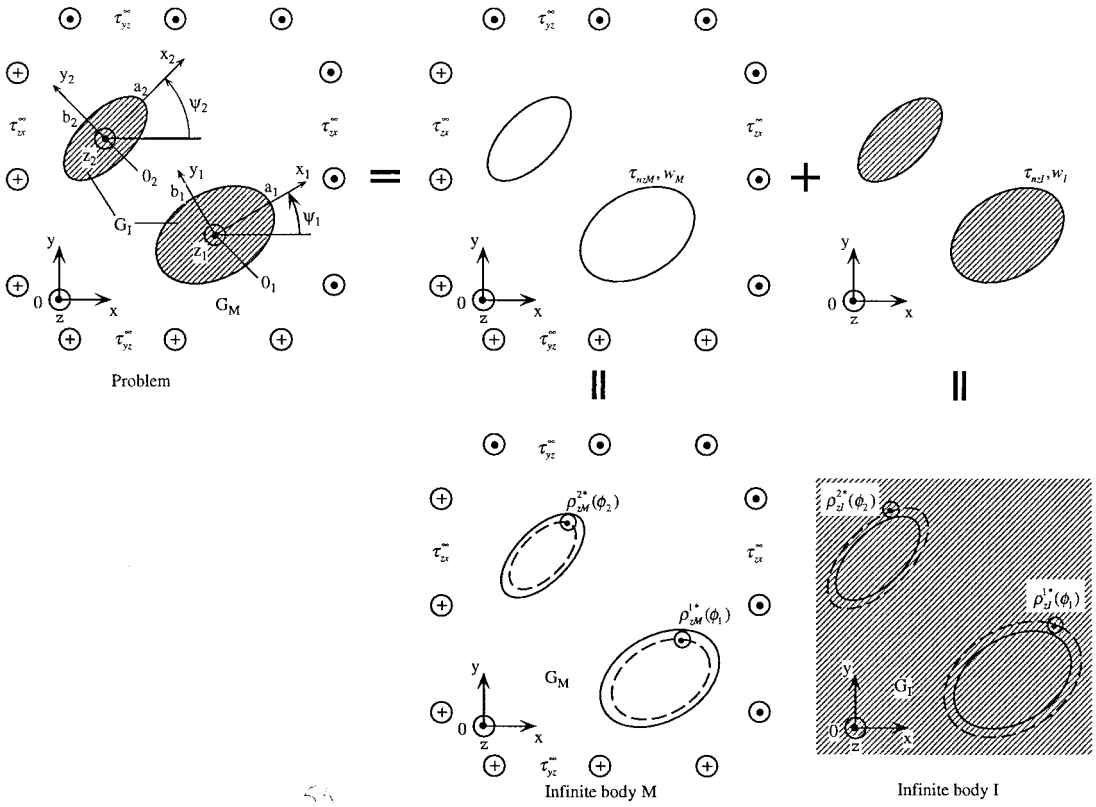

Figure 1. Arbitrarily distributed elliptical inclusions.

2. Numerical solution for singular integral equations under longitudinal shear loading

By taking an example of elliptical inclusions in an infinite body under longitudinal shear τ_{zx}^{∞}, τ_{yz}^{∞} shown in Fig. 1, the present method will be explained. The problem can be formulated in terms of singular integral equations by using the stress field at an arbitrary point (x_i, y_i) when a point force acts on another point (ξ_k, η_k) in an infinite body. The formation is simply based on the principle of the superposition. Consider two infinite bodies. An infinite body 'M' has the same elastic constants as the ones of the matrix, and an infinite body 'I' has the same elastic constants as the ones of inclusions. Denote τ_{nzM}, w_M as stress and displacement which appear along the prospective elliptical boundaries in the infinite body 'M'. In a similar way, denote τ_{nzI}, w_I as stress and displacement which appear along the prospective elliptical boundary in the infinite body 'I'. Then Equations (1) and (2) enforce the boundary conditions at the i-th elliptical boundary; that is, $\tau_{nzM} - \tau_{nzI} = 0$, $w_M - w_I = 0$.

$$
\begin{aligned}
&-(1/2)\rho_{zM}^{i*}(\theta_i) - (1/2)\rho_{zI}^{i*}(\theta_i) \\
&\quad + \sum_{k=1}^{m} \int_0^{2\pi} K_{nzM}^{Fz}(\phi_k,\ \theta_i)\rho_{zM}^{k*}(\phi_k)\ \mathrm{d}s - \sum_{k=1}^{m} \int_0^{2\pi} K_{nzI}^{Fz}(\phi_k,\ \theta_i)\rho_{zI}^{k*}(\phi_k)\ \mathrm{d}s \\
&= -\tau_{nzM}^{\infty} + \tau_{nzI}^{\infty} \\
&\quad [= -(\tau_{zxM}^{\infty}\cos\theta'_{i0} + \tau_{yzM}^{\infty}\sin\theta'_{i0}) + (\tau_{zxI}^{\infty}\cos\theta'_{i0} + \tau_{yzI}^{\infty}\sin\theta'_{i0})]
\end{aligned}
$$

$$
i = 1 \sim m,\ 0 \leqslant \theta_i \leqslant 2\pi, \tag{1}
$$

$$
\sum_{k=1}^{m} \int_0^{2\pi} K_{wM}^{Fz}(\phi_k,\ \theta_i)\rho_{zM}^{k*}(\phi_k)\ \mathrm{d}s - \sum_{k=1}^{m} \int_0^{2\pi} K_{wI}^{Fz}(\phi_k,\ \theta_i)\rho_{zI}^{k*}(\phi_k)\ \mathrm{d}s = -w_M^{\infty} + w_I^{\infty}
$$

$$
i = 1 \sim m,\ 0 \leqslant \theta_i \leqslant 2\pi. \tag{2}
$$

Here, ds is an infinitesimal arc length. $\theta'_{i0} = \theta_{i0} + \psi_i$; θ_{i0} is the angle between x-axis and the normal direction at the point $(x_i,\ y_i)$ on the i-th ellipse, ψ_i is the angle between x_i-axis and x-axis. In Equations (1) and (2), the unknown functions are the body force density $\rho_{zM}^{k*}(\phi_k)$ $(k = 1,\ \ldots,\ m)$ which is distributed in the infinite body 'M', and the density $\rho_{zI}^{k*}(\phi_k)$ $(k = 1,\ \ldots,\ m)$ which is distributed in the infinite body 'I'. Here, m is the number of inclusions and ϕ_k is the angle that specifies the points where body forces are distributed. The function $K_{nzM}^{Fz}(\phi_k, \theta_i)$ means the shear stress induced at the point when the body force with unit density in the z-direction is acting at the infinitesimal arc length on the k-th elliptical boundary. Equations (1) and (2) include Cauchy-type and logarithmic-type singularities, respectively when $i = k$. Therefore when $\theta = \phi$ and $k = i$, the integration in Equation (1) should be interpreted as the meaning of Cauchy's principle values. The unknown functions $\rho_{zM}^{k*}(\phi_k)$ and $\rho_{zI}^{k*}(\phi_k)$ in Equations (1) and (2) are expressed by the following equations.

$$
\rho_{zM}^{k*} = \frac{\mathrm{d}F_{zM}^{k*}}{\mathrm{d}s},\ \rho_{zI}^{k*} = \frac{\mathrm{d}F_{zI}^{k*}}{\mathrm{d}s}. \tag{3}
$$

Here, taking $\mathrm{d}F_{zM}^{k*}$ for example, the notation is the component of the resultant of the body force in the z-direction acting on the infinitesimal arc length ds of matrix. To solve Equations (1) and (2) is to determine the body force densities $\rho_{zM}^{k*}(\phi_k)$, $\rho_{zI}^{k*}(\phi_k)$ in the range $0 \leqslant \phi_k \leqslant 2\pi$. Here, by taking an example of $\rho_{zM}^{k*}(\phi_k)$ how to determine unknown functions will be explained. Consider the auxiliary functions $\rho_{z1M}^{k*}(\phi_k) \sim \rho_{z4M}^{k*}(\phi_k)$ defined by Equation (4) instead of $\rho_{zM}^{k*}(\phi_k)$.

$$
\begin{aligned}
\rho_{z1M}^{k*}(\phi_k) &= \{\rho_{zM}^{k*}(\phi_k) + \rho_{zM}^{k*}(\pi - \phi_k) + \rho_{zM}^{k*}(\pi + \phi_k) + \rho_{zM}^{k*}(-\phi_k)\}/4, \\
\rho_{z2M}^{k*}(\phi_k) &= \{\rho_{zM}^{k*}(\phi_k) + \rho_{zM}^{k*}(\pi - \phi_k) - \rho_{zM}^{k*}(\pi + \phi_k) - \rho_{zM}^{k*}(-\phi_k)\}/4, \\
\rho_{z3M}^{k*}(\phi_k) &= \{\rho_{zM}^{k*}(\phi_k) - \rho_{zM}^{k*}(\pi - \phi_k) - \rho_{zM}^{k*}(\pi + \phi_k) + \rho_{zM}^{k*}(-\phi_k)\}/4, \\
\rho_{z4M}^{k*}(\phi_k) &= \{\rho_{zM}^{k*}(\phi_k) - \rho_{zM}^{k*}(\pi - \phi_k) + \rho_{zM}^{k*}(\pi + \phi_k) - \rho_{zM}^{k*}(-\phi_k)\}/4.
\end{aligned} \tag{4}
$$

These new functions must satisfy Equation (5) because of definition (4).

$$\rho_{z1M}^{k*}(\phi_k) = \rho_{z1M}^{k*}(\pi - \phi_k) = \rho_{z1M}^{k*}(\pi + \phi_k) = \rho_{z1M}^{k*}(-\phi_k),$$

$$\rho_{z2M}^{k*}(\phi_k) = \rho_{z2M}^{k*}(\pi - \phi_k) = -\rho_{z2M}^{k*}(\pi + \phi_k) = -\rho_{z2M}^{k*}(-\phi_k),$$

$$\rho_{z3M}^{k*}(\phi_k) = -\rho_{z3M}^{k*}(\pi - \phi_k) = -\rho_{z3M}^{k*}(\pi + \phi_k) = \rho_{z3M}^{k*}(-\phi_k),$$

$$\rho_{z4M}^{k*}(\phi_k) = -\rho_{z4M}^{k*}(\pi - \phi_k) = \rho_{z4M}^{k*}(\pi + \phi_k) = -\rho_{z4M}^{k*}(-\phi_k). \tag{5}$$

We should note that determining four auxiliary functions $\rho_{z1M}^{k*}(\phi_k) \sim \rho_{z4M}^{k*}(\phi_k)$ in the range $0 \leqslant \phi_k \leqslant \pi/2$, is equivalent to determining original unknown density $\rho_{zM}^{k*}(\phi_k)$ in the range $0 \leqslant \phi_k \leqslant 2\pi$. In other words, if the auxiliary functions $\rho_{z1M}^{k*}(\phi_k) \sim \rho_{z4M}^{k*}(\phi_k)$ are given in the range $0 \leqslant \phi_k \leqslant \pi/2$, original unknown function $\rho_{zM}^{k*}(\phi_k)$ is expressed in the range $0 \leqslant \phi_k \leqslant 2\pi$ using Equation (6).

$$\rho_{zM}^{k*}(\phi_k) = \rho_{z1M}^{k*}(\phi_k) + \rho_{z2M}^{k*}(\phi_k) + \rho_{z3M}^{k*}(\phi_k) + \rho_{z4M}^{k*}(\phi_k),$$

$$\rho_{zM}^{k*}(\pi - \phi_k) = \rho_{z1M}^{k*}(\phi_k) + \rho_{z2M}^{k*}(\phi_k) - \rho_{z3M}^{k*}(\phi_k) - \rho_{z4M}^{k*}(\phi_k),$$

$$\rho_{zM}^{k*}(\pi + \phi_k) = \rho_{z1M}^{k*}(\phi_k) - \rho_{z2M}^{k*}(\phi_k) - \rho_{z3M}^{k*}(\phi_k) + \rho_{z4M}^{k*}(\phi_k),$$

$$\rho_{zM}^{k*}(-\phi_k) = \rho_{z1M}^{k*}(\phi_k) - \rho_{z2M}^{k*}(\phi_k) + \rho_{z3M}^{k*}(\phi_k) - \rho_{z4M}^{k*}(\phi_k). \tag{6}$$

The fundamental density functions for longitudinal shear problem are defined by the following Equation (7). Here, it should be noted that $w_{z3}(\phi_k)$ is the exact density to express a single elliptical inclusion. Equations (7) are good examples of continuous auxiliary functions (4) because they satisfy Equations (5).

$$w_{z1}(\phi_k) = n_z(\phi_k)/\cos\ \phi_k,$$

$$w_{z2}(\phi_k) = n_z(\phi_k)\ \tan\ \phi_k,$$

$$w_{z3}(\phi_k) = n_z(\phi_k),$$

$$w_{z4}(\phi_k) = n_z(\phi_k)\ \sin\ \phi_k. \tag{7}$$

Here, $n_z(\phi_k)$ is the x_k component of the normal unit vector at the point $(x_k,\ y_k)$ on the prospective boundary, and is expressed by the following equation.

$$n_z(\phi_k) = \frac{b_k\ \cos\ \phi_k}{\sqrt{a_k^2\ \sin^2\ \phi_k + b_k^2\ \cos\ \phi_k}} = \cos\ \theta_{k0}. \tag{8}$$

The fundamental density functions defined by Equations (7) are shown in Fig. 2 for a circular boundary. Using Equations (7), original body force densities are expressed as shown in Equation (9).

$$\rho_{z1M}^{k*}(\phi_k) = \rho_{z1M}^{k}(\phi_k) w_{z1}(\phi_k),$$

$$\rho_{z2M}^{k*}(\phi_k) = \rho_{z2M}^{k}(\phi_k) w_{z2}(\phi_k),$$

$$\rho_{z3M}^{k*}(\phi_k) = \rho_{z3M}^{k}(\phi_k) w_{z3}(\phi_k),$$

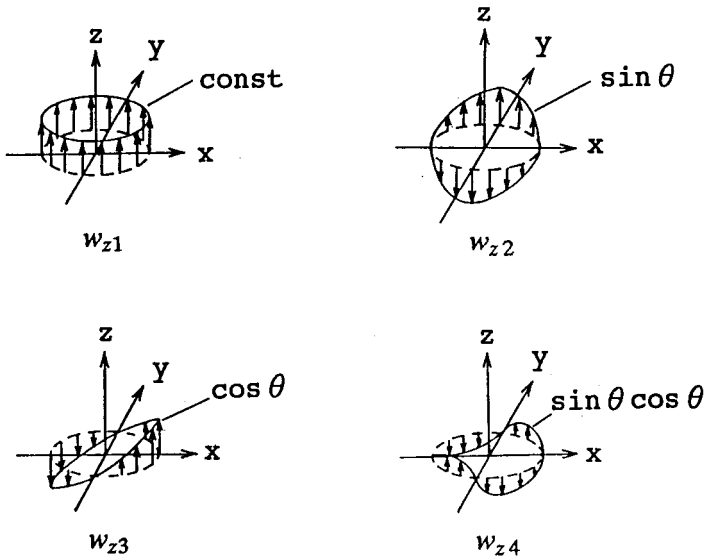

Figure 2. Fundamental density functions for circular boundary.

$$\rho_{z4M}^{k*}(\phi_k) = \rho_{z4M}^{k}(\phi_k) w_{z4}(\phi_k), \tag{9}$$

where $\rho_{z1M}^{k}(\phi_k) \sim \rho_{z4M}^{k}(\phi_k)$ are new unknown functions, which have been called weight functions. Then, all $\rho_{z1M}^{k}(\phi_k) \sim \rho_{z4M}^{k}(\phi_k)$ must satisfy Equation (10).

$$f(\phi_k) = f(\pi - \phi_k) = f(\pi + \phi_k) = f(-\phi_k). \tag{10}$$

Finally, original unknown densities $\rho_{zM}^{k*}(\phi_k)$ can be expressed in Equation (11) as a linear combination of the fundamental densities and the weight functions. The discussion for $\rho_{zI}^{k*}(\phi_k)$ can be made in a similar way of $\rho_{zM}^{k*}(\phi_k)$.

$$\rho_{zM}^{k*}(\phi_k) = \rho_{zM1}^{k}(\phi_k) w_{z1}(\phi_k) + \rho_{zM2}^{k}(\phi_k) w_{z2}(\phi_k) + \rho_{zM3}^{k}(\phi_k) w_{z3}(\phi_k) + \rho_{zM4}^{k}(\phi_k) w_{z4}(\phi_k),$$

$$\rho_{zI}^{k*}(\phi_k) = \rho_{zI1}^{k}(\phi_k) w_{z1}(\phi_k) + \rho_{zI2}^{k}(\phi_k) w_{z2}(\phi_k) + \rho_{zI3}^{k}(\phi_k) w_{z3}(\phi_k) + \rho_{zI4}^{k}(\phi_k) w_{z4}(\phi_k). \tag{11}$$

Here, all unknown weight functions can be approximated as shown in Equations (12) and (13). The expressions satisfy Equation (10).

$$\rho_{z1M}^{k}(\phi_k) = \sum_{n=1}^{M/4} a_{nM}^{k} t_n(\phi_k), \;\; \rho_{z2M}^{k}(\phi_k) = \sum_{n=1}^{M/4} b_{nM}^{k} t_n(\phi_k),$$

$$\rho_{z3M}^{k}(\phi_k) = \sum_{n=1}^{M/4} c_{nM}^{k} t_n(\phi_k), \;\; \rho_{z4M}^{k}(\phi_k) = \sum_{n=1}^{M/4} d_{nM}^{k} t_n(\phi_k),$$

$$\rho_{z1I}^{k}(\phi_k) = \sum_{n=1}^{M/4} a_{nI}^{k} t_n(\phi_k), \;\; \rho_{z2I}^{k}(\phi_k) = \sum_{n=1}^{M/4} b_{nI}^{k} t_n(\phi_k),$$

$$\rho_{z3I}^{k}(\phi_k) = \sum_{n=1}^{M/4} c_{nI}^{k} t_n(\phi_k), \;\; \rho_{z4I}^{k}(\phi_k) = \sum_{n=1}^{M/4} d_{nI}^{k} t_n(\phi_k), \tag{12}$$

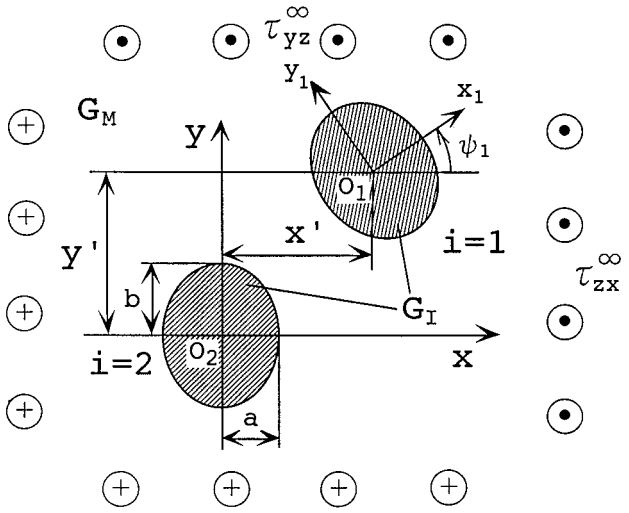

Figure 3. Two equal elliptical inclusions. $i = 1$: $x = a \cos\theta_1 \cos\psi_1 - b \sin\theta_1 \sin\psi_1 + x'$ $y = a \cos\theta_1 \sin\psi_1 + b \sin\theta_1 \cos\psi_1 + y'$ $i = 2$: $x = a \cos\theta_2$, $y = b \sin\theta_2$.

$$t_n(\phi_k) = \cos\{2(n-1)\phi_k\}, \tag{13}$$

where M is the number of the collocation points in $0 \leqslant \phi_k \leqslant 2\pi$. Using the approximation method mentioned above, we obtain the following system of linear equations for determining the coefficients $a_{nM}^k, b_{nM}^k, \ldots, d_{nI}^k$ $(k = 1, \ldots, m)$.

$$\sum_{k=1}^{m}\sum_{n=1}^{M/4} a_{nM}^k A_{nM} + b_{nM}^k B_{nM} + c_{nM}^k C_{nM} + d_{nM}^k D_{nM} + a_{nI}^k A_{nI} + b_{nI}^k B_{nI} + c_{nI}^k C_{nI} + d_{nI}^k D_{nI} = -\tau_{nzM}^{\infty} + \tau_{nzI}^{\infty}, \tag{14}$$

$$\sum_{k=1}^{m}\sum_{n=1}^{M/4} a_{nM}^k E_{nM} + b_{nM}^k F_{nM} + c_{nM}^k G_{nM} + d_{nM}^k H_{nM} + a_{nI}^k E_{nI} + b_{nI}^k F_{nI} + c_{nI}^k G_{nI} + d_{nI}^k H_{nI} = -w_M^{\infty} + w_I^{\infty}, \tag{15}$$

$$A_{nM} = -(1/2)t_n(\theta_i) \cos\theta_{i0}/\cos\theta_i + \int_0^{2\pi} K_{nzM}^{Fz}(\phi_k, \theta_i) t_n(\phi_k) b_k \, \mathrm{d}\phi_k. \tag{16}$$

The notations $B_{nM} \sim H_{nI}$ can be expressed in a similar manner. The stresses at an arbitrary point are represented by a linear combination of the coefficients $a_{nM}^k \sim d_{nI}^k$ $(k = 1, \ldots, m)$ which is determined from the boundary conditions at suitably chosen collocation points and the influence coefficients corresponding to $A_{nM} \sim H_{nI}$. Using the numerical method mentioned above, we will discuss interaction effects of arbitrarily distributed elliptical inclusions under longitudinal shear loading.

Table 1. Maximum stress along the matrix interface of the central inclusion in Fig. 7 under $\tau_{zx}^{\infty} = 0$, $\tau_{yz}^{\infty} = 1$ ($a/b = 1$, $S_{\max} = \tau_{tzM\ \max}/\tau_{tzM0}$ or $S_{\max} = \tau_{nz\ \max}/\tau_{nz0}$, $\tau_{tzM0} = \tau_{tzM\ \max}|_{a/d\to 0}$, $\tau_{nz0} = \tau_{nz\ \max}|_{a/d\to 0}$)

G_I/G_M	a/d	0.0		0.0		0.2		0.4		0.6		0.8	
	N	(deg.)	τ_{tzM0}	(deg.)	$s_{\max}$	(deg.)	$s_{\max}$	(deg.)	$s_{\max}$	(deg.)	$s_{\max}$	(deg.)	$s_{\max}$
	6	0,180	±2.000	0.180	1.000	0.0	1.027	0.0	1.128	0.0	1.384	0.0	2.147
	7	0,180	±2.000	0,180	1.000	0,180	1.029	0.180	1.134	0,180	1.400	0.180	2.204
0.0	8	0,180	±2.000	0,180	1.000	0.0	1.029	0.0	1.137	0.0	1.414	0.0	2.261
	∞		±2.000		1.000		1.035		1.164		1.511		2.706
					(1.000)		(1.035)		(1.164)		(1.511)		(2.705)
	6	0,180	±1.333	0,180	1.000	0.0	1.009	0.0	1.040	0.0	1.107	0.0	1.252
	7	0,180	±1.333	0,180	1.000	0,180	1.009	0,180	1.041	0,180	1.111	0.180	1.258
0.5	8	0,180	±1.333	0,180	1.000	0.0	1.010	0.0	1.042	0.0	1.113	0.0	1.265
	∞		±1.333		1.000		1.011		1.050		1.132		1.307

	N	(deg.)	τ_{nz0}	(deg.)	$s_{\max}$	(deg.)	$s_{\max}$	(deg.)	$s_{\max}$	(deg.)	$s_{\max}$	(deg.)	$s_{\max}$
	6	±90.0	±1.333	±90.0	1.000	±90.0	0.992	±90.0	0.969	±90.0	0.941	±90.1	0.914
	7	±90.0	±1.333	±90.0	1.000	±90.0	0.991	±90.0	0.968	±90.0	0.938	±90.0	0.911
2.0	8	±90.0	±1.333	±90.0	1.000	±90.0	0.991	±90.0	0.967	±90.0	0.937	±90.0	0.908
	∞		±1.333		1.000		0.989		0.961		0.924		0.888
	6	±90.0	±2.000	±90.0	1.000	±90.0	0.975	±90.0	0.913	±90.0	0.844	±90.1	0.790
∞	7	±90.0	±2.000	±90.0	1.000	±90.0	0.974	±90.0	0.910	±90.0	0.838	±90.0	0.782
	8		±2.000	±90.0	1.000	±90.0	0.973	±90.0	0.908	±90.0	0.835	±90.1	0.778
	∞				1.000		0.969		0.892		0.807		0.74

Table 2. Maximum stress along the matrix interface of the outermost inclusion ($j = 1$) in Fig. 7 under $\tau_{zx}^{\infty} = 0$, $\tau_{yz}^{\infty} = 1$ ($a/b = 1$, $S_{\max} = \tau_{tzM\ \max}/\tau_{tzM0}$ or $S_{\max} = \tau_{nz\ \max}/\tau_{nz0}$, $\tau_{tzM0} = \tau_{tzM\ \max}|_{a/d\to 0}$, $\tau_{nz0} = \tau_{nz\ \max}|_{a/d\to 0}$)

G_I/G_M	a/d	0.0		0.0		0.2		0.4		0.6		0.8	
	N	(deg.)	τ_{tzM0}	(deg.)	$s_{\max}$	(deg.)	$s_{\max}$	(deg.)	$s_{\max}$	(deg.)	$s_{\max}$	(deg.)	$s_{\max}$
	6	0.180	±2.000	0.180	1.000	0.0	1.018	0.0	1.093	0.0	1.305	0.0	1.951
0.0	7	0.180	±2.000	0.180	1.000	0.0	1.018	0.0	1.095	0.0	1.31O	0.0	1.975
	8	0.180	±2.000	0.180	1.000	0.0	1.018	0.0	1.096	0.0	1.314	0.0	1.993
	∞		±2.000		1.000		1.020		1.104		1.340		2.109
	6	0.180	±1.333	0.180	1.000	0.0	1.006	0.0	1.029	0.0	1.086	0.0	1.215
05	7	0.180	±1.333	0.180	1.000	0.0	1.006	0.0	1.030	0.0	1.087	0.0	1.217
	8	0.180	±1.333	0.180	1.000	0.0	1.006	0.0	1.030	0.0	1.088	0.0	1.219
	∞		±1.333		1.000		1.006		1.032		1.093		1.231
	N	(deg.)	τ_{nz0}	(deg.)	$s_{\max}$	(deg.)	$s_{\max}$	(deg.)	$s_{\max}$	(deg.)	$s_{\max}$	(deg.)	$s_{\max}$
	6	0.180	±1.333	±90.0	1.000	±90.1	0.995	±90.6	0.983	±91.6	0.967	±92.9	0.952
2.0	7	0.180	±1.333	±90.0	1.000	±90.1	0.995	±90.6	0.982	±91.7	0.966	±92.9	0.951
	8	0.180	±1.333	±90.0	1.000	±90.1	0.995	±90.6	0.982	±91.7	0.965	±92.9	0.950
	∞		±1.333		1.000		0.995		0.980		0.962		0.944
	6	0.180	±2.000	±90.0	1.000	±90.3	0.986	±91.8	0.952	±94.3	0.914	±96.6	0.887
∞	7	0.180	±2.000	±90.0	1.000	±90.3	0.986	±91.8	0.951	±94.3	0.912	±96.7	0.885
	8	0.180	±2.000	±90.0	1.000	±90.3	0.986	±91.8	0.950	±94.3	0.911	±96.7	0.883
	∞		±2.000		1.000		0.984		0.946		0.903		0.872

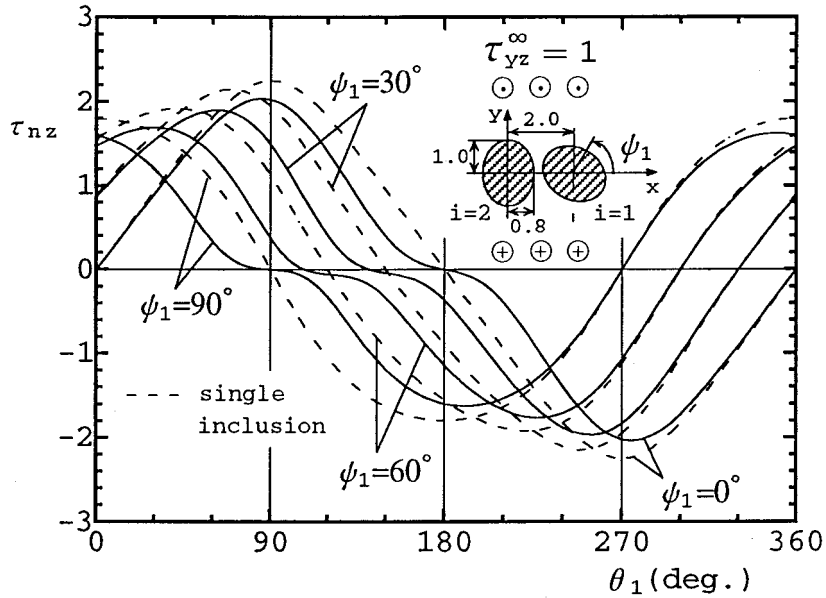

Figure 4. Stress (τ_{nz}) distribution along boundary $i = 1$ ($a = 0.8$, $b = 0.9$, $x' = 2.0$, $y' = 0.0$, $\tau_{zx}^{\infty} = 0$, $\tau_{yz}^{\infty} = 1$, $G_I/G_M = 10^5$ in Fig. 3).

3. Numerical results and discussion

3.1. Results of two elliptical inclusions

The interaction problem of equally shaped two elliptical inclusions in an infinite body under uniform z-direction shear stress $\tau_{zx}^{\infty} = 1$, $\tau_{yz}^{\infty} = 1$ is shown in Fig. 3. The stress distribution τ_{nz} is shown in Fig. 4 when the inclination angle ψ_1 is changed as $\psi_1 = 0°, 30°, 60°, 90°$. It is found that the interaction effect is the largest when two inclusions are extremely close to each other.

Next, we consider two cases, problems A and B, in Fig. 3. Problem A is two inclusions when $\tau_{zx}^{\infty} = 0$, $\tau_{yz}^{\infty} = 1$, $G_I/G_M = C$, and problem B is two inclusions when $\tau_{zx}^{\infty} = 1$, $\tau_{yz}^{\infty} = 0$, $G_I/G_M = 1/C$, both having same geometry, $a = 0.8$, $b = 0.9$, $x' = 2.0$, $y' = 1.0$ (C is a constant and $C > 1$). Figures 5 and 6 show the stress distribution along the boundary of inclusion $i = 1$. Evidently, in Fig. 5(a) and Fig. 6(b) stress distribution τ_{nz} of problem A and stress distribution τ_{tzM} of problem B coincide with each other completely. In addition, in Fig. 5(b) and Fig. 6(a) the absolute values of τ_{tzM} of problem A and that of τ_{nz} of problem B coincide with each other completely.

3.2. Results of a row of elliptical inclusions

A row of elliptical inclusions in an infinite body under longitudinal shear τ_{zx}^{∞}, τ_{yz}^{∞} is shown in Fig. 7. In the following analysis, the maximum stress along the matrix interface of the central and outermost inclusion are calculated. Table 1 shows the values of $S_{\max}$ at the central inclusions and Table 2 shows the values of $S_{\max}$ at the outermost inclusion ($j = 1$) when $\tau_{zx}^{\infty} = 0$, $\tau_{yz}^{\infty} = 1$ with varying the number of inclusion N and a/d. When $G_I/G_M < 1$, the values of $S_{\max}$ mean the dimensionless factor $S_{\max} = \tau_{tzM\ \max}/\tau_{tzM0}$, where $\tau_{tzM\ \max}$ denotes the maximum stress at each inclusion and τ_{tzM0} denotes the maximum stress of a

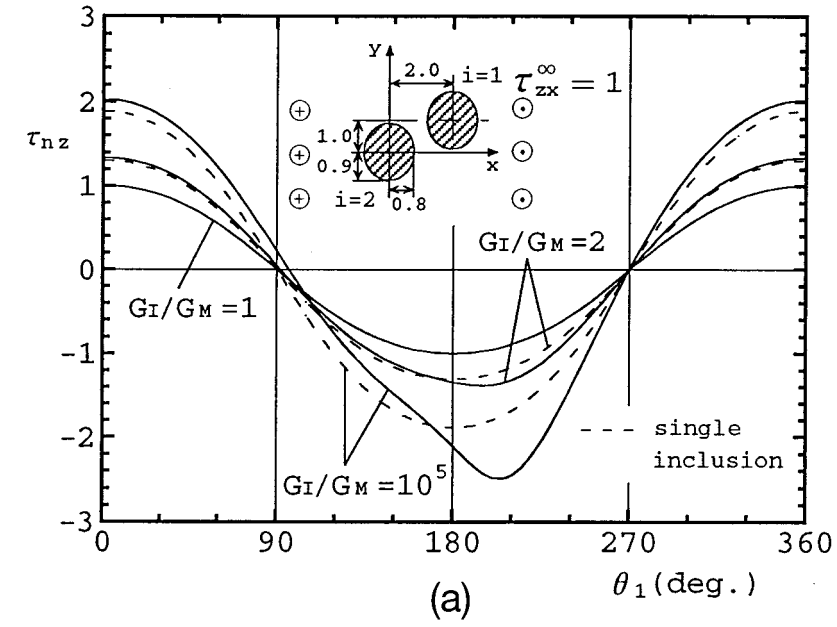

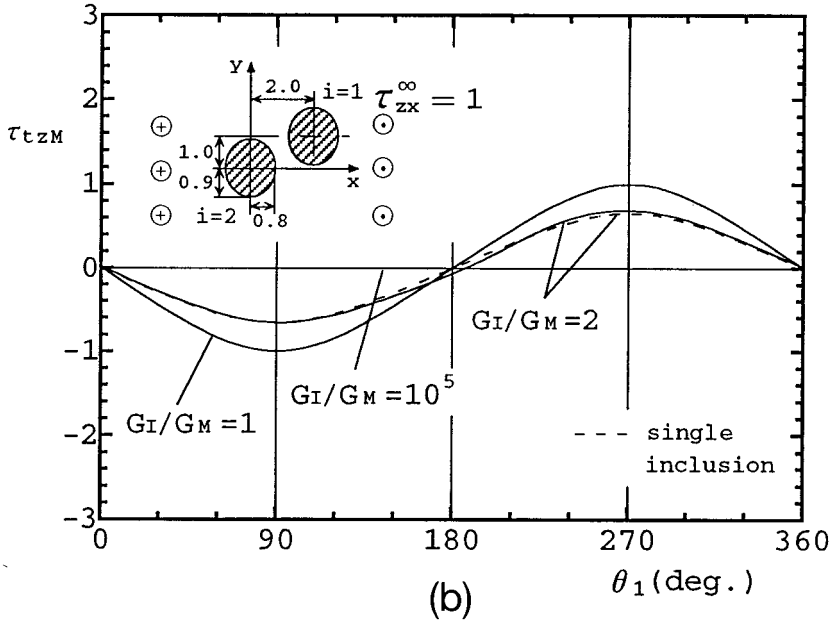

Figure 5. Stress distribution along boundary $i = 1$ ($a = 0.8$, $b = 0.9$, $x' = 2.0$, $y' = 0.0$, $\psi_1 = 0°$, $\tau_{zx}^{\infty} = 1$, $\tau_{yz}^{\infty} = 0$ in Fig. 3). (a) τ_{nz}, (b) τ_{tzM}.

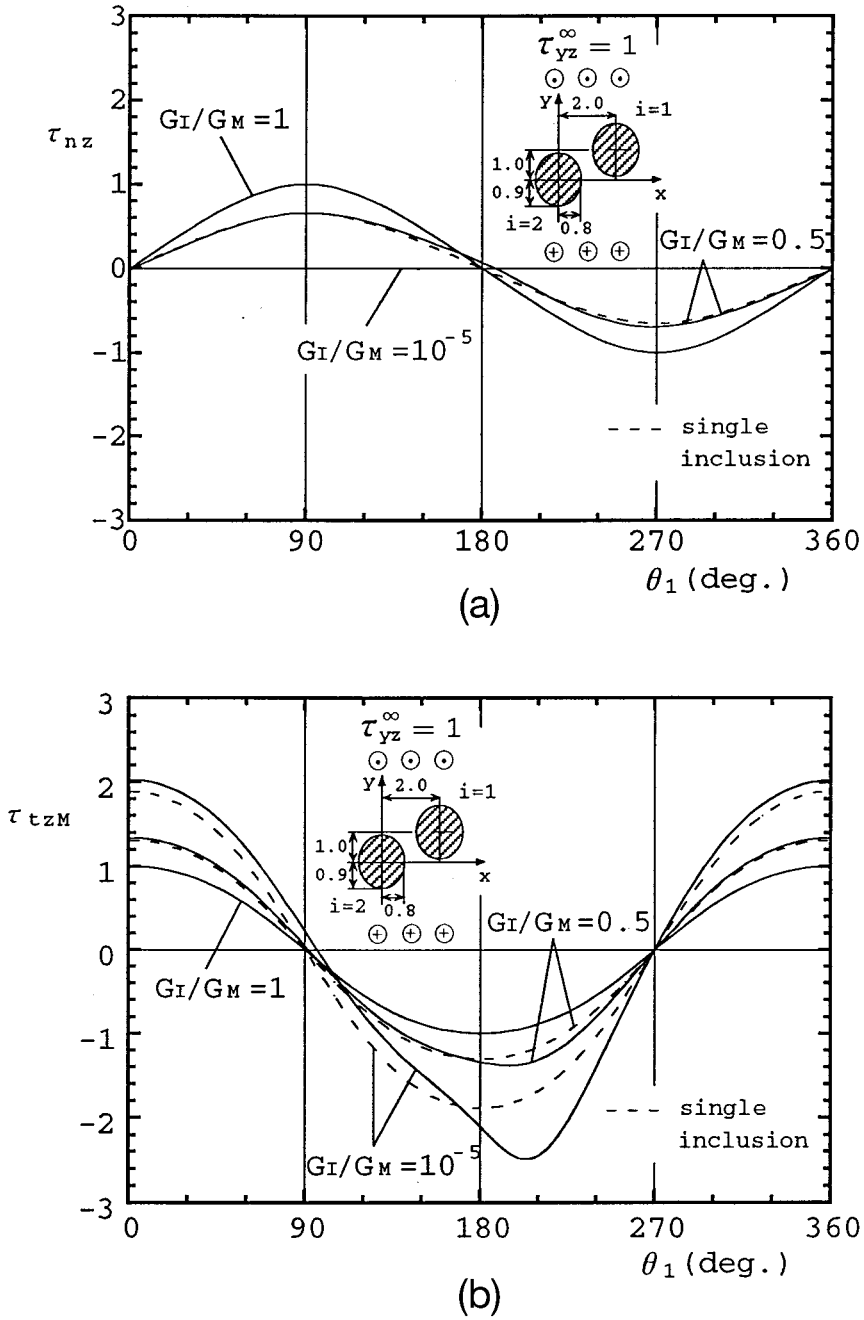

Figure 6. Stress distribution along boundary $i = 1$ ($a = 0.8$, $b = 0.9$, $x' = 2.0$, $y' = 0.0$, $\psi_1 = 0°$, $\tau_{zx}^{\infty} = 0$, $\tau_{yz}^{\infty} = 1$ in Fig. 3). (a) τ_{nz}, (b) τ_{tzM}.

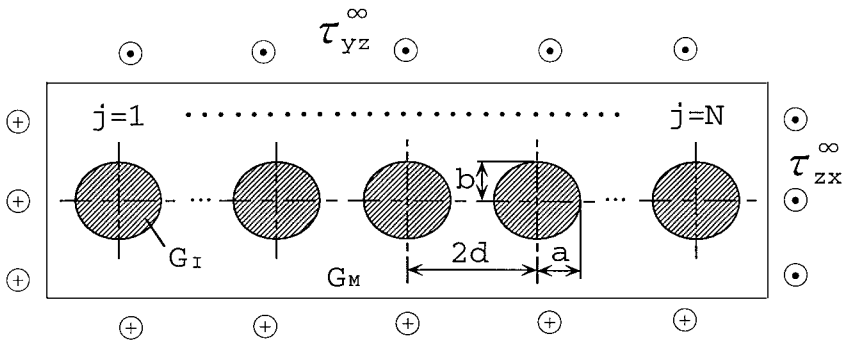

Figure 7. A row of elliptical inclusions.

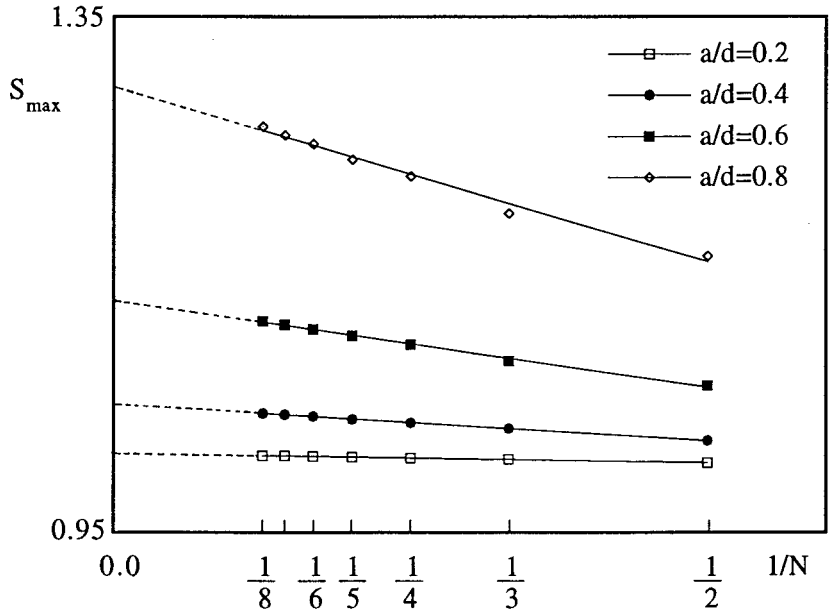

Figure 8. $S_{\max}$ vs $1/N$ relation ($a/b = 1$, $\tau_{zx}^{\infty} = 0$, $\tau_{yz}^{\infty} = 1$, $G_I/G_M = 0.5$).

single circular inclusion. When $G_I/G_M > 1$, the values of $S_{\max}$ mean dimensionless factor $S_{\max} = \tau_{nz\ \max}/\tau_{nz0}$, where $\tau_{nz\ \max}$ denotes the maximum stress at each inclusion and τ_{nz0} denotes the maximum stress of a single circular inclusion. For a row of circular holes, present results and Nisitani's results [7] coincide with each other completely. Fig. 8 shows the relationship between $S_{\max}$ and $1/N$ when $G_I/G_M = 0.5$, $\tau_{zx}^{\infty} = 0$, $\tau_{yz}^{\infty} = 1$ with varying the number of inclusion N and a/d. The values of $S_{\max}$ mean the dimensionless factor $S_{\max} = \tau_{tzM\ \max}/\tau_{tzM0}$, where $\tau_{tzM\ \max}$ denotes the maximum stress at each inclusion and τ_{tzM0} denotes the maximum stress of a single circular inclusion. The present results indicate that the values of $S_{\max}$ are nearly proportional to $1/N$.

4. Conclusions

In this paper, the interaction effect of arbitrarily distributed elliptical inclusions are discussed under longitudinal shear. The conclusions are summarized as follows:

(1) The interaction problem of elliptical inclusions under longitudinal shear was formulated in terms of singular integral equations with the Cauchy-type and logarithmic-type singularities. To formulate the problem, the body force method was applied, where the Green's functions for a point force was used as the fundamental solutions.

(2) The unknown functions of the body force densities were approximated by a linear combination of the fundamental density functions and weight functions. To satisfy the boundary condition, four kinds of fundamental density functions were proposed. It was found that smooth stress distributions were calculated along the boundary.

(3) Interaction of two elliptical inclusions in an infinite body under τ_{zx}^{∞} and τ_{yz}^{∞} was considered. It was found that the stress distribution of τ_{nz} when $\tau_{zx}^{\infty} = 1$, $\tau_{yz}^{\infty} = 0$, $G_I/G_M = C$ (C: constant, $C > 1$) and that of τ_{tzM} when $\tau_{zx}^{\infty} = 0$, $\tau_{yz}^{\infty} = 1$, $G_I/G_M = 1/C$ coincide with each other completely.

(4) For a row of circular inclusions, the maximum stress was found to be nearly proportional to the reciprocal of the number of inclusions. By using the relationships, the extreme values of maximum stress were estimated.

References

1. Donnel, L. H. (1974). *Stress Concentration Factors*, (Edited by R. E. Peterson), John Wiley and Sons, New York, 223.
2. Eshelby, J. D. (1941). The determination of the elastic field of an ellipsoidal inclusion, and related problems. *Proceeding Royal Society London* **A241**, 376–396.
3. Eshelby, J. D. (1959). The elastic field outside an ellipsoidal inclusion. *Proceedings Royal Society London* **A252**, 561–569.
4. Nisitani, H. (1967). The two-dimensional stress problem solved using an electric digital computer. *Journal of Japan Society of Mechanical Engineers* **70**, 627–632 (*Bull. Japan Society of Mechanical Engineers* **11**, 14–23).
5. Nisitani, H. (1974). Solutions of Notch Problems by Body Force Method. In: *Stress Analysis of Notch Problem*, (Edited by G. C. Sih), Leiden, 1–68.
6. Noda, N.-A. and Matsuo, T. (1998). Singular integral equation method for interaction between elliptical inclusions. *ASME Journal of Applied Mechanics* **65**, 310–319.
7. Noda, N.-A., Arita, T. and Matsuo, T. (1997). Numerical solution of singular integral equations of the body force method in stress concentration problems for longitudinal shear loading. *Transactions of the Japan Society of Mechanical Engineers* **63**, 2155–2158.